JOURNAL OF SOLID STATE CHEMISTRY 68, 38–44 (1987)

Lithium and Sodium Insertion Reactions of Phosphate Tungsten Bronzes

E. WANG AND M. GREENBLATT

Department of Chemistry, Rutgers, The State University of New Jersey, New Brunswick, New Jersey 08903

Received June 23, 1986

Lithium insertion reactions of monophosphate tungsten bronzes, $(PO_2)_4(WO_3)_{2m}$ and diphosphate tungsten bronzes $K(P_2O_4)_2(WO_3)_{2m}$ indicate that a maximum of two Li/W and one Na/W may be inserted in these materials. The phosphate tungsten bronzes are three-dimensional network structures made up of slabs of ReO_3-type WO_6 octahedra connected by phosphate groups with large interconnected cavities. Ion-exchange reactions of selected members of $K(P_2O_4)_2(WO_3)_{2m}$ show that potassium which occupies the large hexagonal tunnels in the lattice may be exchanged for various alkali metal cations. Upon lithium insertion, the metallic host materials become insulating. This is attributed to the filling of the π^* conduction band formed by the overlap of W t_{2g} – $5d$ and oxygen π – $2p$ orbitals.

Introduction

Reveau and co-workers have reported on a series of new tungsten phosphate bronzes (*1–11*). The monophosphate tungsten bronzes (MPTB), $(PO_2)_4(WO_3)_{2m}$ form one of the series whose framework is built up from ReO_3-type slabs of WO_6 octahedra interconnected by PO_4 tetrahedra. Empty pentagonal tunnels form at the junction of the ReO_3-type slabs and the slices of tetrahedra as shown in Fig. 1 for the $m = 4$ member (*5*). The structure is similar to γ-Mo_4O_{11} (*12*). Different members of the series differ by the length of the ReO_3-like chains (indicated by the value of m) which run in a zig-zag fashion parallel to the c axis. The diphosphate tungsten bronzes (DPTB), $A_x(P_2O_4)_2(WO_3)_{2m}$ (A = Na, K, Rb, Tl) form a closely related series in which the framework is built up from blocks of corner sharing WO_6 octahedra joined by P_2O_7 diphosphate tetrahedra creating distorted hexagonal tunnels in which the A cations are located as shown in Fig. 2 for the $m = 8$ member (*2, 3, 13*).

In general the phosphate tungsten bronzes (PTB) are characterized by a three-dimensional network structure with interconnected large tunnels. In addition to the large pentagonal or hexagonal tunnels there are perovskite and perovskitelike cubooctahedral cavities which should allow diffusion of cations in these compounds. Our preliminary investigations of the ion exchange properties $K(P_2O_4)_2(WO_3)_{2m}$ in aqueous solutions (discussed subsequently) confirm fast ionic motion. The electronic transport and magnetic properties indicate that these materials are metallic (*8*). The metallic properties are attributed to delocalized electrons in a partially filled π^* con-

0022-4596/87 $3.00

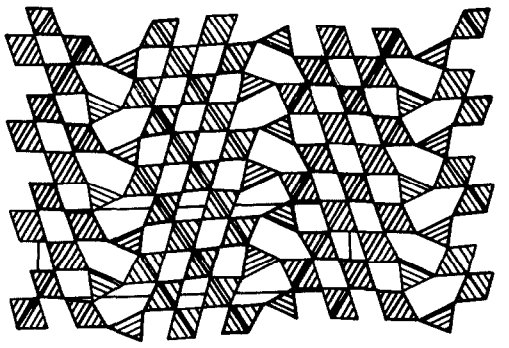

FIG. 1. Schematic projection of the structure of $P_4W_8O_{32}$ ($(PO_2)_4(WO_3)_{2m}$, $m = 4$, MPTB) along the [100] direction (Ref. (*12*)). The unit cell is outlined by the solid line rectangle.

duction band formed by the overlap of tungsten $t_{2g} - 5d$ and oxygen $\pi - 2p$ orbitals.

The structural and electronic properties of the phosphate tungsten bronzes appeared to be well suited for application as cathode materials in secondary batteries and we undertook an investigation of lithium and sodium insertion reactions in selected members of the MPTB and DPTB series.

Experiment

All MPTB and DPTB bronzes in these series were prepared from mixtures of $(NH_4)_2HPO_4$, WO_3, and W or $(NH_4)_2HPO_4$, WO_3, W, and alkali metal carbonates, respectively. In all cases, mixtures of $(NH_4)_2HPO_4$, WO_3, and alkali metal carbonates were first heated to decompose the ammonium phosphates and alkali metal carbonates. Then appropriate amounts of metallic tungsten was added before the mixture was fired in sealed silica tubes. Details of sample preparations were identical to those cited in Refs. (*5*) and (*6*).

Chemical lithiation was carried out by treating the samples with a solution of ~1.5*N* *n*-butyllithium in hexane (*n*-BuLi/hexane) with mechanical stirring for about one week at room temperature. Similarly, sodium insertion was carried out using a solution of ~1.5*N* sodiumnaphthalide in tetrahydrofuran ($NaC_{10}H_8$/THF). The host materials, their alkali metal inserted analogs, and the deintercalated samples were characterized by powder X-ray diffraction with Ni-filtered copper radiation. Qualitative electronic conductivities of the host, Li, and Na inserted phases were measured in a He filled dry box, on thin pellets, which were made by compacting fine powder specimens in a hollow Teflon cylinder with two stainless-steel plungers, which also served as two leads. An 0.1*N* solution of iodine in acetonitrile (I_2/CH_3CN) was used as the deintercalating reagent. The alkali metal stoichiometries of the resulting compounds were determined by titrametric and plasma emission spectroscopic methods.

For the electrochemical studies, cells were constructed using Li metal foil as anode, PTB samples as cathode, and $LiClO_4$ in propylene carbonate ($LiClO_4$/PC) as the liquid electrolyte. A similar attempt was made for the electrochemical insertion of sodium with an analogous Na cell, but the large overpotential (long equilibration time) made such investigation impractical.

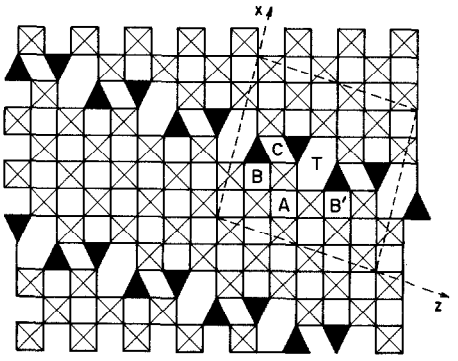

FIG. 2. Projection of the idealized structure of $AP_4W_{16}O_{56}$ along the [010] direction. The different types of cavities in the structure are: tunnels (T) with distorted hexagonal geometry; cubooctahedral cages (A, B) related to perovskitelike cavities; cages (B', C) created by 11 oxygen atoms (Ref. (*13*)).

TABLE I

RESULTS OF Li AND Na INSERTION/EXTRACTION IN SELECTED MPTB ($(PO_2)_4(WO_3)_{2m}$) PHASES

m	Compounds	Color	Lithiated compounds	Li/W inserted	Delithiated compounds	Li/W left	Na^+ compounds	Na/W
4	$P_4W_8O_{32}$	Red	$Li_{15}P_4W_8O_{32}$	1.9	$Li_{1.7}P_4W_8O_{32}$	0.96	$Na_6P_4W_8O_{32}$	0.75
6	$P_4W_{12}O_{44}$	Blue	$Li_{24}P_4W_{12}O_{44}$	2	$Li_{9.4}P_4W_{12}O_{44}$	0.78	$Na_{12}P_4W_{12}O_{44}$	1
7	$P_4W_{14}O_{50}$	Dkblue	$Li_{26}P_4W_{14}O_{50}$	1.9	$Li_{8.5}P_4W_{14}O_{50}$	0.61	$Na_8P_4W_{14}O_{50}$	0.6
8	$P_4W_{16}O_{56}$	Black	$Li_{33}P_4W_{16}O_{56}$	2	$Li_{12}P_4W_{16}O_{56}$	0.76	$Na_{19}P_4W_{16}O_{56}$	1.2
10	$P_4W_{20}O_{68}$	Black	$Li_{39}P_4W_{20}O_{68}$	2	$Li_{12}P_4W_{20}O_{68}$	0.61	$Na_{19}P_4W_{20}O_{68}$	0.95

Thermal analyses of the samples, which were hermetically sealed in aluminum pans inside a helium filled dry box, were carried out on a DuPont 9900 computer controlled thermal analyzer system. After the thermal treatments, samples were examined by X-ray powder diffraction for any structural changes.

Results and Discussion

Using an amount of *n*-BuLi/hexane solution in excess of Li/W = 1 for each PTB, the samples (those that were initially red or blue; Tables I and II) turned brown immediately and then dark blue or black after a few hours. The MPTB bronzes seemed to change color quicker than those of the DPTB series. When sodium insertion was carried out with excess $NaC_{10}H_8$/THF the samples turned black or dark brown. Deintercalation by I_2/CH_3CN did not restore the original color in any of the samples, indicating that some lithium or sodium still remained.

The stoichiometries of the Li and Na inserted bronzes are tabulated in Tables I and II. The MPTB series (Table I) for selected members show a fairly uniform uptake of 2 Li/W. This is similar to the limit of $Li_{2.5}WO_3$ reported in high-temperature (~50°C) reactions of *n*-BuLi with WO_3 (*14*). Similarly, Li_2ReO_3 is the limiting stoichiometry of the reaction of ReO_3 with *n*-BuLi either at room temperature or at 50°C (*15*). In Li_2ReO_3 the cubic structure of ReO_3 distorts to create two octahedral sites in the perovskite cavity to accommodate the two Li^+ ions (*16*). These results are consistent with lithium ions occupying cubooctahedral cavities in the ReO_3-like slabs of the PTB. Alternatively, lithium ions could partially occupy all the available cavities or preferentially be located in just some of them. A

TABLE II

RESULTS OF Li AND Na INSERTION/EXTRACTION IN SELECTED DPTB ($K(P_2O_4)_2(WO_3)_{2m}$) PHASES

m	Compounds[a]	Lithiated compounds	Li/W inserted	Delithiated compounds	Li/W left	Na^+ compounds	Na^+ Na/W
5	$KP_4W_{10}O_{38}$	$Li_{19}KP_4W_{10}O_{38}$	1.9	$Li_8KP_4W_{10}O_{38}$	0.8	$Na_{10}KP_4W_{10}O_{38}$	1
6	$KP_4W_{12}O_{44}$	$Li_{22}KP_4W_{12}O_{44}$	1.8	$Li_{11}KP_4W_{12}O_{44}$	0.9	$Na_8KP_4W_{12}O_{44}$	0.7
7	$KP_4W_{14}O_{50}$	$Li_{26}KP_4W_{14}O_{50}$	1.9	—	—	$Na_6KP_4W_{14}O_{50}$	0.4
8	$KP_4W_{16}O_{56}$	$Li_{30}KP_4W_{16}O_{56}$	1.9	—	—	—	—
10	$KP_4W_{20}O_{68}$	$Li_{35}KP_4W_{20}O_{68}$	1.7	$Li_{10}KP_4W_{20}O_{68}$	0.5	—	—

[a] The color of all DPTB is dark blue or black.

TABLE III

POWDER X-RAY DIFFRACTION PATTERNS OF $P_4W_8O_{32}$ AND ITS Li AND Na INSERTED ANALOGS[a]

	$P_4W_8O_{32}$ (red)		$Li_6P_4W_8O_{32}$ (brown)		$Li_{15}P_4W_8O_{32}$ (black)		$Na_6P_4W_8O_{32}$ (drk brown)	
k k l	d_{obs}(Å)	I/I_0	d_{obs}(Å)	I/I_0	d_{obs}(Å)	I/I_0	d_{obs}(Å)	I/I_0
					10.1	100,b		
0 0 2	8.81	15	8.78	50	8.85	30,b	8.87	30,b
0 1 3	4.35	50	4.35	80	4.35	30	4.38	80,b
1 1 1	4.03	100	3.97	100	4.00	40	4.03	100
1 1 2	3.72	70	3.70	85	3.70	40	3.74	80,b
0 1 4	3.62	45	3.64	50	3.62	25	3.65	40,b
1 1 3	3.37	55	3.34	60	3.35	30	3.38	70,b
1 2 1	2.757	20	2.756	25	2.755	10	2.773	15
1 2 2	2.648	80	2.654	55	2.638	20,b	2.665	80,b
2 0 2	2,547	60	2.538	50	2.533	20	2.544	50

Note. b = broadened.

[a] The average error in d_{obs} is ±0.02 Å.

powder neutron diffraction profile analysis determination of the structure of the lithiated phases might resolve this problem. The results indicate that in general more lithium than sodium can be inserted in the PTB and that about the same amount of lithium can be inserted in the MPTB as in the DPTB (Table I and II). This finding is not surprising, since lithium is considerably smaller than sodium, hence more lithium per unit volume of the cavities might be expected to be inserted. The relatively large scatter of Na/W values observed in the various compounds (Table I and II) is partly due to the viscous nature of the sodiumnaphthalide/THF solution and the difficulty in determining its volume accurately. Since the pentagonal tunnels in the MPTB are empty while the hexagonal tunnels in the DPTB are partially occupied by the K ions, one would expect more lithium/sodium to be inserted in MPTB than in the DPTB if the inserted ions occupy those tunnel sites. However, in DPTB the cavities are considerably larger than in MPTB and the openings of the 3D bottlenecks of the diffusion paths also appear to be larger in DPTB. These factors may account for the observation that equal amounts of alkali metals may be inserted in both. Results of deintercalation by I_2/CH_3CN (Tables I and II) indicate that the reaction is partially irreversible and that there might be some structural changes upon excess (Li/W > 1) intercalation as indicated by additional lines appearing in the powder X-ray diffraction patterns of some of the lithiated MPTB samples. The K ions in DPTB appear to stabilize the structure against decomposition upon lithiation to some extent, as the strong X-ray diffraction line seen at $d \sim 10$ Å in the overlithiated MPTB samples is absent in analogous DPTB samples. Results of partial lithiations seem to indicate that the optimum Li/W ratio is about one.

X-ray powder diffraction patterns of the alkali metal inserted samples generally have broadened peaks and reduced intensities compared to their respective hosts (Table III). For the sodium inserted samples, the X-ray peaks generally shift toward lower 2θ, while for the lithiated samples, the shifts in 2θ are not uniform (Tables III). Partial lithiation reactions of some of the

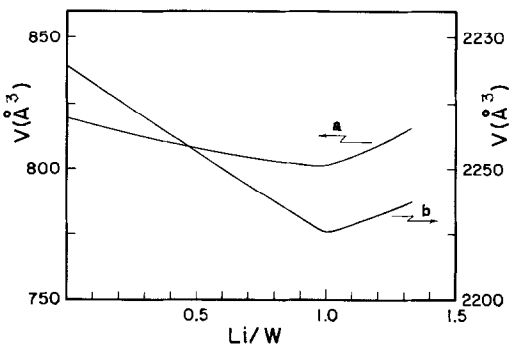

FIG. 3. Variation of unit cell volume with Li/W content: (a) $P_4W_{12}O_{44}$ (MPTB), (b) $KP_4W_{18}O_{62}$ (DPTB).

bronzes indicate that the unit cell volume of the lithiated samples contracts while those of the sodium inserted samples expands compared to that of the hosts. A plot of the unit cell volume of $P_4W_8O_{32}$ (MPTB) and $KP_4W_{18}O_{62}$ (DPTB) vs Li/W (Fig. 3) shows that the volume decreases in both structural types units up to Li/W = 1. For Li/W > 1 the cell volume increases with increasing Li content, but it is still smaller than that of the cell volume of the hosts. Similar results have been seen in other lithiated samples (*15*). The effective ionic radius of Li^+ is considerably smaller (for any coordination number), than that of Na^+ (*17*), hence Li^+ is more polarizing than Na^+. This effect is probably amplified by the big cavities of the hosts. Thus, initially the polarizing Li^+ ions cause the volume of the unit cell to decrease, but as more and more Li^+ ions are inserted, repulsive interactions between neighboring Li^+ become important and at Li/W > 1 an increase in the volume is observed (this may partially or wholly be due to some structural changes that might occur beyond the Li/W > 1 ratio). In the case of sodium insertion, due to the large effective size of Na^+, a steady increase in the volume is seen with increasing Na content.

Electrochemical results show that Li may be inserted up to an Li/W ratio of about one, before any irreversible structural changes occur, in agreement with chemical lithiation results. The discharge curves indicate a continuous single phase with increasing Li in the range $0 < Li/W < 1$ for both $P_4W_8O_{32}$ (MPTB) and $KP_4W_{12}O_{44}$ (DPTB) (Fig. 4). Charging was done for the $P_4W_8O_{32}$ cell and some irreversibility is indicated, which was also confirmed by the iodine delithiation results (Table I). This partial irreversibility may be due to inher-

TABLE IV

LATTICE PARAMETERS OF SELECTED PHOSPHATE TUNGSTEN BRONZES AND THEIR Li AND Na INSERTED ANALOGS[a]

Compds	a(Å)	b(Å)	c(Å)	β	V(Å³)
$P_4W_8O_{32}$	5.32	6.52	17.45	90	605.7
$Li_6P_4W_8O_{32}$	5.19	6.61	17.44	90	598.2
$Li_{12}P_4W_8O_{32}$	5.23	6.59	17.39	90	599.9
$Li_{15}P_4W_8O_{32}$	5.23	6.60	17.37	90	599.5
$Na_6P_4W_8O_{32}$	5.32	6.54	17.68	90	615.1
$P_4W_{12}O_{44}$	5.30	6.56	23.54	90	818.4
$Li_{11}P_4W_{12}O_{44}$	5.21	6.53	23.58	90	802.5
$Li_{16}P_4W_{12}O_{44}$	5.26	6.54	23.70	90	816.1
$Na_{12}P_4W_{12}O_{44}$	5.32	6.66	23.95	90	847.4
$P_4W_{14}O_{50}$	5.30	6.54	26.69	90	924.4
$Li_{14}P_4W_{14}O_{50}$	5.27	6.61	26.38	90	914.3
$Na_8P_4W_{14}O_{50}$	5.36	6.58	27.04	90	953.6
$KP_4W_{12}O_{44}$	14.01	7.53	17.06	114.3	1639
$Li_{22}KP_4W_{12}O_{44}$	14.04	7.50	16.95	114.5	1624
$Na_8KP_4W_{12}O_{44}$	14.04	7.50	17.09	114.4	1639
$KP_4W_{14}O_{50}$	14.62	7.51	17.09	99.0	1842
$Li_{17}KP_4W_{14}O_{50}$	14.73	7.52	16.84	99.3	1842
$Na_6KP_4W_{14}O_{50}$	14.72	7.50	16.8	99.2	1833
$KP_4W_{18}O_{62}$	18.14	7.53	17.12	101.5	2289
$Li_{18}KP_4W_{18}O_{62}$	17.81	7.48	16.98	100.5	2225
$Li_{24}KP_4W_{18}O_{62}$	17.84	7.50	17.01	100.6	2237
$KP_4W_{10}O_{58}$	11.20	7.51	17.13	93.5	1438
$Li_8KP_4W_{10}O_{38}$	11.07	7.49	16.99	93.9	1406
$Li_{15}KP_4W_{10}O_{38}$	11.11	7.51	16.95	93.9	1410
$Li_{19}KP_4W_{10}O_{38}$	11.13	7.49	16.96	93.8	1412
$Na_{10}KP_4W_{10}O_{38}$	11.27	7.51	17.09	93.5	1443

[a] esd in a, b, c, and V are ±0.02, ±0.02, ±0.05 Å, and ±0.2 Å³, respectively, in the $(PO_2)_4(WO_3)_{2m}$ phases. Corresponding esd in a, b, c, and V are ±0.02, ±0.01, ±0.02 Å, and ±0.3 Å³ in the $K(P_2O_4)_2(WO_3)_{2m}$ (DPTB) compounds.

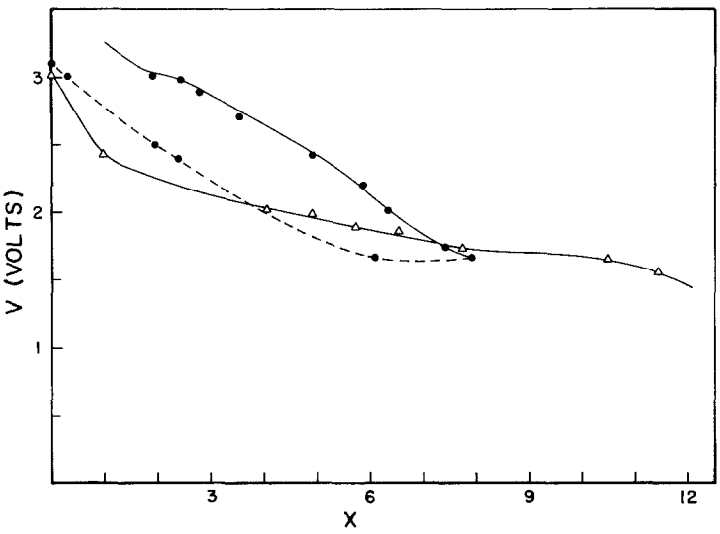

FIG. 4. Charge (dashed line) and discharge (solid line, ● are experimental data) curves of a small test cell Li/$LiClO_4$, PC/$P_4W_8O_{32}$; solid line with △ experimental data is the discharge curve of $KP_4W_{12}O_{44}$ (DPTB). x is the atomic lithium content in $Li_xP_4W_8O_{32}$ and $Li_xKP_4W_{12}O_{44}$, respectively.

ent defects, including shearing of the ReO_3-type regions due to missing P_2O_7 or disordered stacking of the ReO_3 slabs present in the host materials as observed by high-resolution electron microscopy (*18, 19*). From the discharge curves, one notes that the emf decreases slowly and is high up to the reversible limit of Li content in the PTB. This property is useful for battery applications.

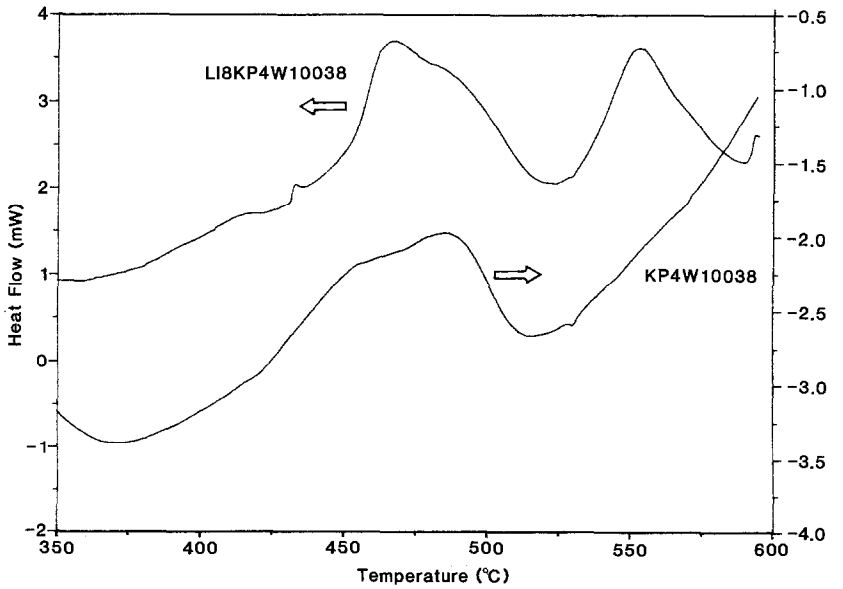

FIG. 5. Differential scanning calorimetic results of $KP_4W_{10}O_{38}$ (DPTB) and its lithiated analog $Li_8KP_4W_{10}O_{38}$.

Qualitative resistivity measurements show that the resistivities of the inserted samples are larger than their corresponding host materials by at least two orders of magnitude. Since the host materials are metallic conductors, alkali metal insertion presumably results in the filling of the W–O–W hybridized π^* conduction band and the concomitant change from metal to semiconductor or to insulating properties.

Ion exchange reactions in aqueous solutions of RbOH and NaOH, respectively, were carried out on $KP_4W_{10}O_{38}$ (DPTB) and $K_{1.5}P_4W_{16}O_{56}$ (DPTB) samples. Elemental analysis of the samples by plasma emission spectroscopy shows that very little (<0.02 mole) Rb, but ~0.4 mole of Na exchange for K, respectively. Furthermore, ~0.3 mole of K can be extracted with I_2/CH_3CN. This indicates that the K ions are fairly mobile in the DPTB phases.

Thermal analysis was done in order to see if any difference in tightness of bonding between the host and the different types of inserted compounds might be observed by their decomposition temperatures. In all cases (Fig. 5) the decomposition temperature was found to be ~500°C or higher, but no significant differences in the decomposition temperature of the sodium and lithium inserted compounds were found. An exothermic peak seen at ~430°C in $KP_4W_{10}O_{38}$ (MPTB) and in its lithiated analog may be similar in nature to that of the 480°C peak observed in $NaP_4W_{12}O_{44}$ (MPTB), which was attributed to a structural phase transition in that compound (*8*).

Acknowledgments

We thank F. Rinaldi for help with the preparation of several of the host compounds. This research received partial support from the Office of Naval Research, National Science Foundation–Solid State Chemistry Program, Grant DMR-84-04003, and National Science Foundation–Materials Research Instrument, Grant DMR-84-08266.

References

1. J. P. GIROULT, M. GOREAUD, PH. LABBE, AND B. RAVEAU, *Acta Crystallogr. B* **37,** 2139 (1981).
2. J. P. GIROULT, M. GOREAUD, PH. LABBE, AND B. RAVEAU, *Acta Crystallogr. B* **37,** 1163 (1981).
3. J. P. GIROULT, M. GOREAUD, PH. LABBE, AND B. RAVEAU, *Acta Crystallogr. B* **36,** 2570 (1980).
4. J. P. GIROULT, M. GOREAUD, PH. LABBE, AND B. RAVEAU, *J. Solid State Chem.* **44,** 407 (1984).
5. B. DOMENGES, F. STUDER, AND B. RAVEAU, *Mat. Res. Bull.* **18,** 669 (1983).
6. A. BENMOUSSA, D. GIROULT, PH. LABBE, AND B. RAVEAU, *Acta Crystallogr.* **40,** 573 (1984).
7. M. HERVIEU AND B. RAVEAU, *J. Solid State Chem.* **43,** 299 (1982).
8. M. BERMOUSSA, D. GIROULT, AND B. RAVEAU, *Rev. Chim. Min.* **21,** 710 (1984).
9. PH. LABBE, D. OUACHEE, M. GOREAUD, AND B. RAVEAU, *J. Solid State Chem.* **50,** 163 (1983).
10. J. P. GIROULT, M. GOREAUD, PH. LABBE, AND B. RAVEAU, *Rev. Chim. Min.* **20,** 829 (1983).
11. B. DOMENGES, M. GOREAUD, PH. LABBE, AND B. RAVEAU, *J. Solid State Chem.* **50,** 173 (1983).
12. L. KIHLBORG, *Arkiv Kemi* **21,** 365 (1963).
13. J. P. GIROULT, M. GOREAUD, J. PROVOST, PH. LABBE, AND B. RAVEAU, *Mat. Res. Bull.* **16,** 811 (1981).
14. K. H. CHENG AND M. S. WHITTINGHAM, *Solid State Ionics* **1,** 151 (1980).
15. D. W. MURPHY, M. GREENBLATT, R. J. CAVA, AND S. M. ZAHURAK, *Solid State Ionics* **5,** 327 (1981).
16. R. J. CAVA, A. J. SANTORO, D. W. MURPHY, S. ZAHURAK, AND R. S. ROTH, *Solid State Ionics* **5,** 323 (1981).
17. R. D. SHANNON, *Acta Crystallogr. A* **32,** 751 (1976).
18. M. HERVIEU, B. DOMENGES, AND B. RAVEAU, *J. Solid State Chem.* **58,** 233 (1985).
19. M. HERVIEU AND B. RAVEAU, *Chem. Scripta* **22,** 117 (1985).